arXiv:1009.3886v1 [hep-ph] 20 Sep 2010

Lepton Flavour Violating τ and μ decays induced by scalar leptoquark

Rachid Benbrik,[1, 2, 3] Mohamed Chabab,[1] and Gaber Faisel[4, 5]

[1]*LPHEA, Department of Physics, FSSM, Cadi Ayyad University,*
P.O.B. 2390, Marrakech 40 000, Morocco.
[2] *Department of Physics, National Cheng-Kung University, Tainan 701, Taiwan*
[3] *National Center for Theoretical Sciences, Hsinchu 300, Taiwan.*
[4] *Egyptian Center for Theoretical Physics,*
Modern University for Information and Technology ,
Faculty of Engineering, AlHadaba AlWusta, AlMokattam, Cairo, Egypt.
[5] *Faculty of education, Thamar University, Yemen.*

(Dated: September 21, 2010)

Abstract

We show that the scalar leptoquark Yukawa couplings generate a significant lepton flavour violation. We compute the light scalar leptoquark contributions to the branching ratios (Br) of the lepton flavour violating (LFV) decays $\ell \to \ell_i \ell_j \bar{\ell}_j$ and $\ell \to \ell' \gamma$ with (i,j = e,μ). We discuss the role of the relevant input parameters to these decay rates which are the Yukawa couplings ($h_{a\ell}$) with ($a = u, c, t$), the light scalar mass M_{S_1} and the mixing angle $\sin 2\theta_{LQ}$. We investigate the experimental limits from $(g-2)_\mu$, $\mu - e$ conversion and $\pi \to e\nu_e, \mu\nu_\mu$ to get constraint on the input parameter space. We predict that the upper limits on the branching ratios of $\tau \to \ell_i \ell_j \bar{\ell}_j$ can reach the experimental current limits. We also show that it is possible to accommodate both $\tau \to \ell_i \ell_j \bar{\ell}_j$ and $\tau \to \ell\gamma$ branching ratios for certain choices of LQ parameters.

PACS numbers: 13.35.Dx, 13.20.-v,13.35.-r, 14.60.Hi

I. INTRODUCTION

Lepton-flavor violation (LFV), if observed in a future experiment, is an evidence of new physics beyond the standard model, because the lepton-flavor number is conserved in the standard model. Since the processes are theoretically free from the non perturbative hadronic effects they provide accurate predictions for the decay rates and the branching ratios (Br) of these processes. Furthermore, they are theoretically rich as they carry considerable information about the free parameters of the used model. On the other hand, the experimental work which has been done regarding these decays motivates their theoretical studies. For instance, experimental prospect for $\mu \to e\gamma$ is promising with the recent commencement of the MEG experiment which will probe $\mathrm{Br}(\mu \to e\gamma) \approx 10^{-13}$ two orders of magnitude beyond the current limit. B factories search for the decay mode $\tau \to \ell_i \ell_j \bar{\ell}_j$ at the e^+e^- experiment with upper limits in the range $\mathrm{Br}(\tau \to \ell_i \ell_j \bar{\ell}_j) \leq (2-8) \times 10^{-8}$ [1]. Searches for $\tau \to \mu\mu\bar{\mu}$ can be performed at the Large Hadron Collider (LHC) where τ leptons are copiously produced from the decays of W, Z, B and D, with anticipated sensitivities to $\mathrm{Br}(\tau \to \mu\mu\bar{\mu}) \approx 10^{-8}$ [2]. The decay $\mu \to ee\bar{e}$ of which there is a strict bound $\mathrm{Br}(\mu \to ee\bar{e}) \leq 10^{-12}$ is a strong constraint on the parameter space [3].

The present experimental upper limits for the branching ratios of $\ell \to \ell_i \ell_j \bar{\ell}_j$ and $\ell \to \ell' \gamma$ decays are given by [1, 3]

$$\mathrm{Br}(\tau \to \ell_i \ell_j \bar{\ell}_j) \sim 10^{-8}, \qquad \mathrm{Br}(\mu \to \bar{e}ee) \sim 10^{-12}, \tag{1}$$

and [4–6]

$$\begin{aligned} \mathrm{Br}(\tau \to \mu\gamma) &< 6.8 \times 10^{-8}, \\ \mathrm{Br}(\tau \to e\gamma) &< 1.1 \times 10^{-7}, \\ \mathrm{Br}(\mu \to e\gamma) &< 1.2 \times 10^{-11}. \end{aligned} \tag{2}$$

Within the SM, the Brs of LFV decays are extremely small. On the other hand, the difference between the experimental value of the muon anomalous magnetic moment $a_\mu = (g-2)/2$ and its SM prediction is given by[7–9]

$$\Delta a_\mu = a_\mu^{\mathrm{exp}} - a_\mu^{\mathrm{SM}} = (29.5 \pm 8.8) \times 10^{-10}, \tag{3}$$

with a discrepancy of 3.4 σ. In spite of the substantial progress in both experimental and theoretical sides, the situation is not completely clear yet. However, the possibility that the present discrepancy may arise from the errors in the determination of the hadronic leading-order contribution to Δa_μ seems to be unlikely as argued in Ref. [10]. There are many attempts, in the literature, to explain this discrepancy through considering new physics beyond SM [11–13].

One of the possibilities for physics beyond the Standard Model is the four-color symmetry between quarks and leptons introduced by Pati-Salam [14]. The prediction of the existence of gauge leptoquarks, which are rather heavy according to the current available data, is a direct consequence of this symmetry.

The current bounds on the leptoquarks production are set by Tevatron, LEP and HERA [15]. Tevatron experiments have set limits on the scalar leptoquarks masses $M_{LQ} >$ 242 GeV. On the other hand, the limits that have been set by LEP and HERA experiments are model dependent. The search for these novel particles will be continued at the CERN LHC. Preliminary studies at the LHC experiments, ATLAS [16] and CMS [17], indicate that clear signals can be observed for masses up to 1.2 TeV.

Our aim in this paper is to analyze the branching ratios for all processes given in Eqs.(1)-(2) in the context of the LQ model. These LFV processes are generated at loop level through exchanging scalar LQ particles which transmit the lepton flavour mixing from the Yukawa couplings to the observed charged lepton sector. Previous studies of such decays were performed extensively by theorists [18]. In the present study of these decay channels, the light scalar leptoquark effects to $\ell \to \ell_i \ell_j \bar{\ell}_j$ are discussed in detail, namely the contributions of the photon and Z boson penguins and box diagrams. Also, we include the predictions for $\ell \to \ell_i \ell_i \bar{\ell}_i$ channels correlated with $\ell \to \ell' \gamma$ rates which are interesting within the framework we use. Furthermore, we take into account $(g-2)_\mu$, $\mu - e$ conversion and $\pi \to e\nu_e, \mu\nu_\mu$ constraints imposed on the input parameter space. This is carried here by considering the parametrization introduced in [19] for the case of the $\ell \to \ell_i \ell_j \bar{\ell}_j$ decays.

The paper is organized as follows: In Section II, we list the relevant terms of the scalar leptoquark Lagrangian to the LFV decays and the analytical expressions of the scalar leptoquark contributions to a_μ and $\ell \to \ell' \gamma$ decays. The analytical results of the LFV decays $\ell \to \ell_i \ell_j \bar{\ell}_j$ will be presented in Sec.III. In Sec.IV, we derive the constraints that can be imposed on some leptoquark Yukawa couplings obtained using $\mu - e$ conversion. The numerical results for τ and μ decays will be presented in Sec.V. Finally, Sec.VI will be devoted to the conclusion.

II. LEPTOQUARK BASICS

A. Scalar Leptoquark Interactions

In this section we list the relevant terms of the scalar leptoquark Lagrangian to our LFV decay modes. We consider isosinglet scalar leptoquarks. The effective Lagrangian that describes the leptoquark interactions in the mass basis can be written as [20, 21]:

$$\begin{aligned}\mathcal{L}_{LQ} &= \overline{u_a^c}\Big(h'_{ai}\Gamma_{k,S_R}P_L + h_{ai}\Gamma_{k,S_L}P_R\Big)e_i S_k^* + \overline{e_j}\Big(h'^*_{aj}\Gamma^\dagger_{S_R,k}P_R + h^*_{aj}\Gamma^\dagger_{S_L,k}P_L\Big)u_a^c S_k \\ &- eQ_{(u^c)}A_\mu\overline{u_a^c}\gamma^\mu u_a^c - ieQ_S A_\mu S_k^*\overleftrightarrow{\partial^\mu}S_k + ieQ_S\tan\theta_W Z_\mu S_k^*\overleftrightarrow{\partial^\mu}S_k \\ &- \frac{e}{s_W c_W}Z_\mu\overline{u_a^c}\gamma^\mu\Big((T_{3(u^c)} - Q_{(u^c)}s_W^2)P_R - Q_{(u^c)}s_W^2 P_L\Big)u_a^c,\end{aligned} \tag{4}$$

where $k = 1, 2$ are the leptoquark indices, $T_3 = -1/2$, $Q_{u^c} = -2/3$ are quark's isospin and electric charge respectively, $Q_S = -1/3$ is the electric charge of the scalar leptoquarks S_k, a is up-type quark flavor indices, i, j are lepton flavor indices, $c_W = \cos\theta_W$ and $s_W = \sin\theta_W$. The $\Gamma_{k,S_{L(R)}}$ are elements of leptoquark mixing matrix that bring $S_{L(R)}$ to the mass eigenstate basis S_k:

$$S_L = \Gamma^\dagger_{S_L,k}S_k, \qquad S_R^* = \Gamma_{k,S_R}S_k^*, \tag{5}$$

Here $S_{L(R)}$ denotes the field associated with the $\overline{e_j}P_{L(R)}u_a^c$ terms in $\mathcal{L}_{LQ}$ [20]. Note that in the no-mixing case ($\Gamma = 1$), $S_{1(2)}$ reduce to $S_{L(R)}$ which are called chiral leptoquarks as they only couple to quarks and leptons in certain chirality structures. Finally, the couplings h and h' are 3 by 3 matrices that give rise to various LFV processes and must be subjected to the experimental constraints. In this work we do not intend to explore the effects of all possible leptoquark interactions. Instead, we try to demonstrate that a simple scalar leptoquark model can provide rich and interesting LFV phenomena.

B. Muon anomalous magnetic moment $(g-2)_\mu$

The LQ interaction can generate muon anomalous magnetic moment and resolve the discrepancy between theoretical and experimental results. The corresponding one-loop diagrams are shown in Fig. 1(a)- 1(b) where $\ell = \ell' = \mu$. The extra contribution to a_μ arising

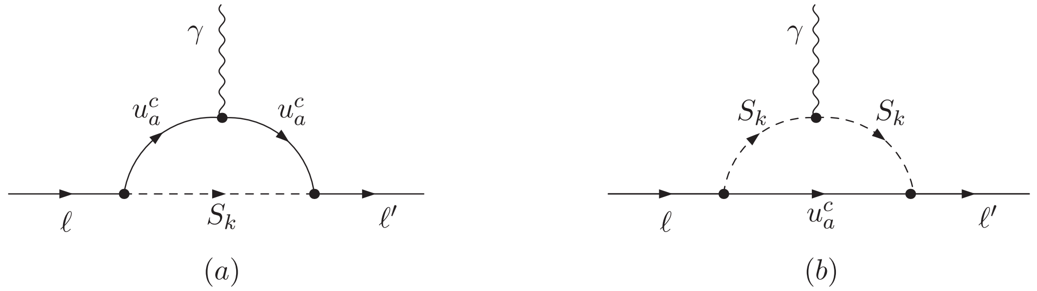

FIG. 1: Feynman diagrams contributing to $\ell \to \ell'\gamma$, S_k denotes the scalar leptoquark with $k = 1, 2$ and u_a^c denotes up-type quark with $a = 1, 2, 3$.

from the LQ model due to quark and scalar leptoquark one-loop contribution is given by

$$a_\mu^{LQ} = -\frac{N_c m_\mu^2}{8\pi^2}\sum_{a=1}^{3}\sum_{k=1}^{2}\frac{1}{M_{S_k}^2}\Bigg[\big(|h_{a\mu}\Gamma_{k,S_L}|^2 + |h'_{a\mu}\Gamma_{k,S_R}|^2\big)\big(Q_{(u^c)}F_2(x_{ka}) - Q_S F_1(x_{ka})\big) - \frac{m_{(u_a^c)}}{m_\mu}\mathrm{Re}\big(h'_{a\mu}h^*_{a\mu}\Gamma^+_{S_R,k}\Gamma_{k,S_L}\big)\big(Q_{(u^c)}F_3(x_{ka}) - Q_S F_4(x_{ka})\big)\Bigg], \qquad (6)$$

In the above expression, $N_c = 3$, $Q_S = -1/3$, $Q_{u^c} = -2/3$. The kinematic loop functions F_i $(i = 1, ..., 4)$ depend on the variable $x_{ka} = m_{(u_a^c)}^2/M_{S_k}^2$, their expressions are given in the appendix B.

Clearly, the use of leptoquark contribution to saturate the deviation shown in Eq.(3) leads to constraint leptoquark masses M_{S_k} (k=1,2), mixing angle θ_{LQ} and the Yukawa couplings $(h_{a\mu},\, h_{a\mu}^{(\prime)})$.

C. $\ell \to \ell'\gamma$

In this subsection, we give the expression for the amplitude of $\ell \to \ell'\gamma$ which is generated by exchange of scalar leptoquark. According to the gauge invariance, the amplitude can be written as:

$$i\mathcal{M}^\gamma = ie\bar{u}(p_2)\bigg(F_{2RL}^\gamma P_L + F_{2LR}^\gamma P_R\bigg)(i\sigma_{\mu\nu}q^\nu)u(p_1)\varepsilon_\gamma^{\mu *}, \qquad (7)$$

where ε_γ is the polarization vector and $q = p_1 - p_2$ is the momentum transfer. For the amplitude of leptoquark exchange at one-loop level, as depicted in Fig. 1 with $\ell \neq \ell'$, we have

$$
\begin{aligned}
F^{\gamma}_{2LR} = \frac{N_c}{16\pi^2}\sum_{a=1}^{3}\sum_{k=1}^{2}\frac{1}{M^2_{S_k}}\Bigg[& \big(m_\ell h'_{a\ell}h'^{*}_{a\ell'}\Gamma^{\dagger}_{S_R,k}\Gamma_{k,S_R} + m_{l'}h_{a\ell}h^{*}_{a\ell'}\Gamma^{\dagger}_{S_L,k}\Gamma_{k,S_L}\big) \\
& \times\big(Q_{(u^c)}F_2(x_{ka}) - Q_S F_1(x_{ka})\big) \\
& - m_{(u^c_a)}\big(h_{a\ell}h'^{*}_{a\ell'}\Gamma^{\dagger}_{S_R,k}\Gamma_{k,S_L}\big)\big(Q_{(u^c)}F_3(x_{ka}) - Q_S F_4(x_{ka})\big)\Bigg], \qquad (8)
\end{aligned}
$$

$$
F^{\gamma}_{2RL} = F^{\gamma}_{2LR}(h \leftrightarrow h', R \leftrightarrow L), \qquad (9)
$$

with $x_{ka} = m^2_{(u^c_a)}/M^2_{S_k}$. The branching ratio of $\ell \to \ell'\gamma$ is given by:

$$
\mathrm{Br}(\ell \to \ell'\gamma) = \frac{\alpha_{em}}{4\Gamma(\ell)}\frac{(m^2_\ell - m^2_{\ell'})^3}{m^3_\ell}\Big(|F^{\gamma}_{2LR}|^2 + |F^{\gamma}_{2RL}|^2\Big), \qquad (10)
$$

In our numerical calculations we analyze the Brs of the decays under consideration by using the total decay widths of the decaying leptons $\Gamma(\ell)$.

III. $\ell^- \to \ell_i^- \ell_j^- \ell_j^+$

In this section, we present the analytical results for the LFV τ decay into three leptons with different flavor within leptoquark model. Next, we give the analytical results relative to the branching ratios of $\tau^- \to \ell_i^- \ell_j^- \ell_j^+$ (the analogous results in the muon sector can be obtained by means of a simple generalization.) We perform a complete one-loop calculation of the τ decay width for all six possible channels, $\tau^- \to \mu^-\mu^-\mu^+$, $\tau^- \to e^-e^-e^+$, $\tau^- \to \mu^-\mu^+e^-$, $\tau^- \to e^-e^+\mu^-$, $\tau^- \to \mu^-\mu^-e^+$ and $\tau^- \to \mu^+e^-e^-$. The contribution generated by the γ-, Z-penguins and box diagrams are presented here separately. Throughout this section we follow closely the notation and thr way of presentation of [22].

First, we define the amplitude for $\tau^-(p) \to \ell_i^-(p_1)\ell_j^-(p_2)\ell_j^+(p_3)$ decays as the sum of the various contributions,

$$
\mathcal{A}(\tau^- \to \ell_i^- \ell_j^- \ell_j^+) = \mathcal{A}_{\gamma-penguin} + \mathcal{A}_{Z-penguin} + \mathcal{A}_{box}. \qquad (11)
$$

In the following subsections, we present the results for these contributions in terms of some convenient form factors.

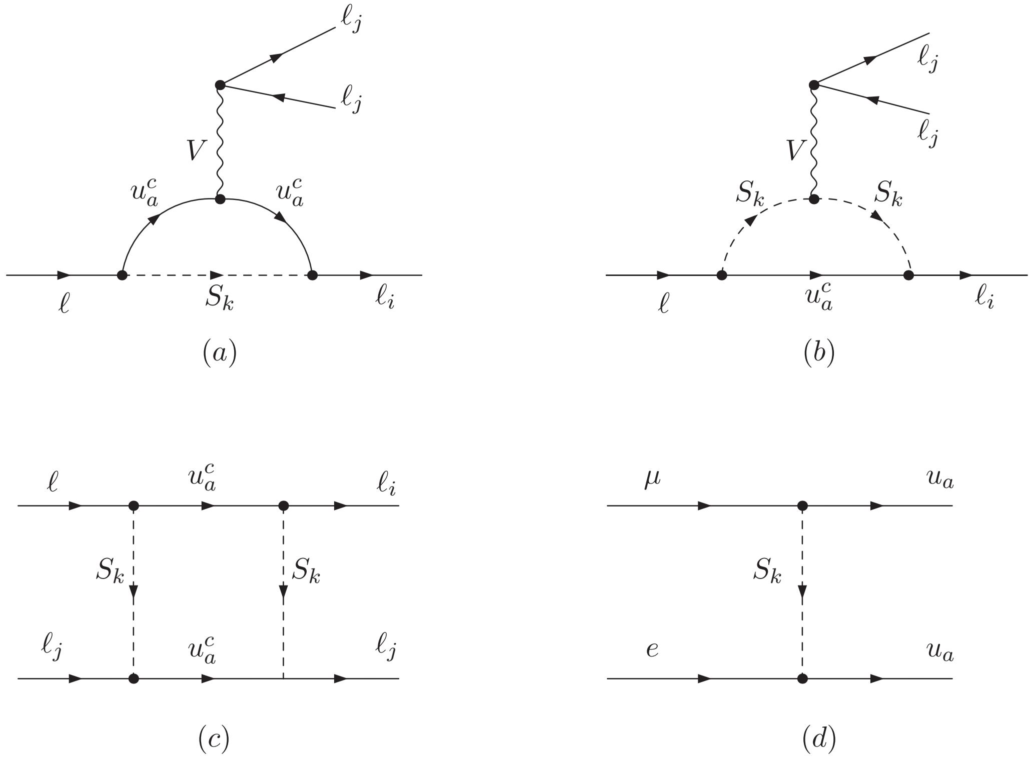

(a) (b) (c) (d)

FIG. 2: Photon (a) and Z-penguin (b) and box (c) Feynman diagrams contributing to $\ell^- \to \ell_i^- \ell_j^- \ell_j^+$, S_k are the scalar leptoquark $k = 1, 2$, u_a^c are type-up quark with $a = 1, 2, 3$. The (d) $(\mu - e)$ conversion Feynman diagram.

A. The γ-penguin contributions

Diagrams in which a photon is exchanged are referred as γ-penguin diagrams and are shown in Figs. 2(a) and 2(b) when $V = \gamma$. The amplitude of $\tau^-(p) \to \ell_i^-(p_1)\ell_j^-(p_2)\ell_j^+(p_3)$ decays can be written as

$$\begin{aligned} i\mathcal{A}_{\gamma-penguin} &= \bar{u}(p_1)\Big[q^2\gamma_\mu(T_1^L P_L + T_1^R P_R) + i m_\tau \sigma_{\mu\nu} q^\nu (T_2^L P_L + T_2^R P_R)\Big]u(p) \\ &\times \frac{e^2}{q^2}\bar{u}(p_2)\gamma^\mu v(p_3), \end{aligned} \tag{12}$$

where q is the photon momentum and e is the electric charge. The photon-penguin amplitude has two contributions, one from Fig. 2(a) and the other from Fig. 2(b) diagrams respectively as can be seen from the structure of the form factors,

$$T_i^{L,R} = T_i^{(a)L,R} + T_i^{(b)L,R}, \qquad \mathrm{i} = 1, 2 \tag{13}$$

$$\begin{aligned}
T_1^{(a)L} &= -\frac{N_c Q_{(u^c)}}{16\pi^2} \sum_{a=1}^{3} \sum_{k=1}^{2} \frac{1}{M_{S_k}^2} h'_{a\tau} h'^*_{ai} \Gamma^\dagger_{S_R,k} \Gamma_{k,S_R} F_5(x_{ka}), && (14)\\
T_2^{(a)L} &= -\frac{N_c Q_{(u^c)}}{16\pi^2} \sum_{a=1}^{3} \sum_{k=1}^{2} \frac{1}{M_{S_k}^2} \Bigg[h_{a\tau} h^*_{ai} \Gamma^\dagger_{S_L,k} \Gamma_{k,S_L} F_1(x_{ka}) + h'_{a\tau} h'^*_{ai} \Gamma^\dagger_{S_R,k} \Gamma_{k,S_R} \frac{m_i}{m_\tau} F_1(x_{ka}) \\
&+ h'_{a\tau} h^*_{ai} \Gamma^\dagger_{S_L,k} \Gamma_{k,S_R} \frac{m_{u_a}}{m_\tau} F_3(x_{ka}) \Bigg] && (15)\\
T_i^{(a)R} &= T_i^{(a)L}(h \leftrightarrow h', R \leftrightarrow L). && (16)
\end{aligned}$$

and,

$$\begin{aligned}
T_1^{(b)L} &= -\frac{N_c Q_S}{16\pi^2} \sum_{a=1}^{3} \sum_{k=1}^{2} \frac{1}{M_{S_k}^2} h'_{a\tau} h'^*_{ai} \Gamma^\dagger_{S_R,k} \Gamma_{k,S_R} F_6(x_{ka}), && (17)\\
T_2^{(b)L} &= \frac{N_c Q_S}{16\pi^2} \sum_{a=1}^{3} \sum_{k=1}^{2} \frac{1}{M_{S_k}^2} \Bigg[h_{a\tau} h^*_{ai} \Gamma^\dagger_{S_L,k} \Gamma_{k,S_L} F_2(x_{ka}) + h'_{a\tau} h'^*_{ai} \Gamma^\dagger_{S_R,k} \Gamma_{k,S_R} \frac{m_i}{m_\tau} F_2(x_{ka}) \\
&+ h'_{a\tau} h^*_{ai} \Gamma^\dagger_{S_L,k} \Gamma_{k,S_R} \frac{m_{u_a}}{m_\tau} F_4(x_{ka}) \Bigg] && (18)\\
T_i^{(b)R} &= T_i^{(b)L}(h \leftrightarrow h', R \leftrightarrow L). && (19)
\end{aligned}$$

where $x_{ka} = m_{u_a}^2 / M_{S_k}^2$. Note that we have not neglected any of the fermion masses. The analytical expressions for the loop functions F_i $(i = 1, ..., 6)$ are given in appendix B.

B. The Z-penguin contributions

In addition to the photon penguin diagrams discussed in the previous subsection, there are other types of penguin diagrams in which the Z boson is exchanged as shown in Figs. 2(a)-2(b). The amplitude in this case can be written as

$$\begin{aligned}
i\mathcal{A}_{Z-penguin} = &\frac{ie^2}{m_Z^2 c_W^2 s_W^2} \bar{u}(p_1) \gamma_\mu \big(Z^L P_L + Z^R P_R\big) u(p) \\
&\times \bar{u}(p_2) \gamma^\mu \big(g_L P_L + g_R P_R\big) v(p_3),
\end{aligned} \tag{20}$$

As before, the coefficient $Z^{L(R)}$ can be written as a sum of two terms from Feynman diagrams in Fig. 2(a) and Fig. 2(b):

$$Z^{L,R} = Z^{(a)L,R} + Z^{(b)L,R} \tag{21}$$

where,

$$\begin{aligned}
Z^{(a)L} &= -\frac{N_c}{16\pi^2}\sum_{a=1}^{3}\sum_{k=1}^{2}\frac{1}{M_{S_k}^2}h'_{a\tau}h'^{*}_{ai}\Gamma^{\dagger}_{S_R,k}\Gamma_{k,S_R}\Bigg[2C_R F_8(x) - m_{u_a}^2 C_L F_7(x_{ka})\Bigg], &(22)\\
Z^{(a)R} &= Z^{(a)L}(h' \to h, R \leftrightarrow L). &(23)\\
Z^{(b)L} &= -\frac{N_c}{16\pi^2}\sum_{a=1}^{3}\sum_{k=1}^{2}\frac{1}{M_{S_k}^2}h'_{a\tau}h'^{*}_{ai}\Gamma^{\dagger}_{S_R,k}\Gamma_{k,S_R}\Bigg[2Q_S\tan\theta_W\Bigg]F_8(x_{ka}), &(24)\\
Z^{(b)R} &= Z^{(b)L}(h' \to h, R \leftrightarrow L). &(25)
\end{aligned}$$

the coefficients $C_{L(R)}$ and $g_{L(R)}$ denote Z boson coupling to charged leptoquark S and charged leptons $l_{L(R)}$, respectively and they are given by

$$\begin{aligned}
g_{L(R)} &= T_{3L(R)} - Q_{em}\sin^2\theta_W, &(26)\\
C_{L(R)} &= T_{3L(R)(u^c)} - Q_{(u^c)}\sin^2\theta_W, &(27)
\end{aligned}$$

where $T_{3L(R)}$ and Q_{em} represent weak isospin and electric charge of $l_{L(R)}$, respectively. The loop functions F_i (i=7,8) are presnted in the appendix B.

C. The box contribution

The amplitude corresponding to the box-type diagram shown in Fig .2(c) can be expressed as,

$$\begin{aligned}
i\mathcal{A}_{box} &= B_1^L[\bar{u}(p_1)\gamma^\mu P_L u(p)][\bar{u}(p_2)\gamma_\mu P_L v(p_3)] + B_1^R[\bar{u}(p_1)\gamma^\mu P_R u(p)][\bar{u}(p_2)\gamma_\mu P_R v(p_3)]\\
&+ B_2^L[\bar{u}(p_1)\gamma^\mu P_L u(p)][\bar{u}(p_2)\gamma_\mu P_R v(p_3)] + B_2^R[\bar{u}(p_1)\gamma^\mu P_R u(p)][\bar{u}(p_2)\gamma_\mu P_L v(p_3)]\\
&+ B_3^L[\bar{u}(p_1)P_L u(p)][\bar{u}(p_2)P_L u(p)] + B_3^R[\bar{u}(p_1)P_R u(p)][\bar{u}(p_2)P_R v(p_3)]\\
&+ B_4^L[\bar{u}(p_1)\sigma^{\mu\nu}P_L u(p)][\bar{u}(p_2)\sigma_{\mu\nu}P_L v(p_3)]\\
&+ B_4^R[\bar{u}(p_1)\sigma^{\mu\nu}P_R u(p)][\bar{u}(p_2)\sigma_{\mu\nu}P_R v(p_3)]. \qquad (28)
\end{aligned}$$

where

$$B_i^{L,R} = B_i^{(c)L,R} \qquad i = 1, ..., 4 \tag{29}$$

with,

$$B_1^{(c)L} = \frac{N_c}{32\pi^2}\sum_{a,a'=1}^{3}\sum_{k,k'=1}^{2}\widetilde{D}_0(m_{u_a}^2, m_{u_{a'}}^2, m_{S_k}^2, m_{S_{k'}}^2)h'_{a\tau}h'_{a'j}h'^*_{ai}h'^*_{a'j}|\Gamma^\dagger_{S_R,k}\Gamma_{k',S_R}|^2, \tag{30}$$

$$\begin{aligned}B_2^{(c)L} &= \frac{N_c}{64\pi^2}\sum_{a,a'=1}^{3}\sum_{k,k'=1}^{2} h'_{a\tau}h_{a'j}\Gamma_{k,S_R}\Gamma_{k',S_L}\Big[h^*_{a'j}h'^*_{ai}\Gamma^\dagger_{S_R,k'}\Gamma^\dagger_{S_L,k}\widetilde{D}_0(m_{u_a}^2, m_{u_{a'}}^2, m_{S_k}^2, m_{S_{k'}}^2)\\ &\quad -m_{u_a}m_{u_{a'}}h'^*_{a'j}h^*_{ai}\Gamma^\dagger_{S_R,k}\Gamma^\dagger_{S_L,k'}D_0(m_{u_a}^2, m_{u_{a'}}^2, m_{S_k}^2, m_{S_{k'}}^2)\Big],\end{aligned} \tag{31}$$

$$\begin{aligned}B_3^{(c)L} &= \frac{N_c}{16\pi^2}\sum_{a,a'=1}^{3}\sum_{k,k'=1}^{2} m_{u_a}m_{u'_a}h'_{a'j}h'_{a\tau}h^*_{ai}h^*_{a'j}\Gamma^\dagger_{S_L,k'}\Gamma_{k,S_R}\Gamma^\dagger_{S_L,k}\Gamma_{k',S_R}\\ &\qquad \times D_0(m_{u_a}^2, m_{u_{a'}}^2, m_{S_k}^2, m_{S_{k'}}^2)\end{aligned} \tag{32}$$

$$B_4^{(c)L} = 0, \tag{33}$$

$$B^{(c)R} = B^{(c)L}(h' \leftrightarrow h, R \leftrightarrow L). \tag{34}$$

Again the loop functions D_0 and $\widetilde{D}_0$ are given in the appendix B.

By collecting all the formulas, the Branching ratios of $\tau^- \to \ell_i^- \ell_j^- \ell_j^+$ can be written in terms of the different form factors as

$$\begin{aligned}\mathrm{Br}(\tau^- \to \ell_{\mathrm{i}}^- \ell_{\mathrm{j}}^- \ell_{\mathrm{j}}^+) &= \frac{\alpha^2 m_\tau^5}{32\pi\Gamma_\tau}\Bigg[|T_1^L|^2 + |T_1^R|^2 + \frac{2}{3}\Big(|T_2^L|^2 + |T_2^R|^2\Big)\Big(8\log\Big(\frac{m_\tau}{2m_i}\Big)-11\Big)\\ &- 2(T_1^L T_2^{R*} + T_2^L T_1^{R*} + \mathrm{h.c}) + \frac{1}{3m_Z^4 s_W^4 c_W^4}\Big(2\big(|Z^L g_L|^2 + |Z^R g_R|^2\big)\\ &+ |Z^L g_R|^2 + |Z^R g_L|^2\Big) + \frac{1}{6}\big(|B_1^L|^2 + |B_1^R|^2\big) + \frac{1}{3}\big(|B_2^L|^2 + |B_2^R|^2\big)\\ &+ \frac{1}{24}\big(|B_3^L|^2 + |B_3^R|^2\big) + \frac{1}{3}\big(T_1^L B_1^{L*} + T_1^L B_2^{L*} + T_1^R B_1^{R*} + T_1^R B_2^{R*} + \mathrm{h.c}\big)\\ &- \frac{2}{3}\big(T_2^R B_1^{L*} + T_2^L B_1^{R*} + T_2^L B_2^{R*} + T_2^R B_2^{L*} + \mathrm{h.c}\big)\\ &+ \frac{1}{3}\big(B_1^L Z_L^* g_L + B_1^R Z_R^* g_R + B_2^L Z_L^* g_R + B_2^R Z_R^* g_L + \mathrm{h.c}\big)\\ &+ \frac{1}{3}\big[2(T_1^L Z_L^* g_L + T_1^R Z_R^* g_R) + T_1^L Z_L^* g_R + T_1^R Z_R^* g_L + \mathrm{h.c}\big]\\ &+ \frac{1}{3}\big[-4(T_2^R Z_L^* g_L + T_2^L Z_R^* g_R) - 2(T_2^L Z_R^* g_L + T_2^R Z_L^* g_R + \mathrm{h.c})\big]\Bigg]\end{aligned} \tag{35}$$

where Γ_τ is the total decay width of τ. All the form factors are real.

IV. $\mu - e$ CONVERSION

$\mu - e$ conversion in the muonic atoms is one of the interesting charged LFV process that can occur in many candidates of physics beyond the SM. Accurate calculation of the $\mu - e$ conversion rate is essential to compare the sensitivity to the LFV interactions in different nuclei [23]. In this section, we discuss the constraints that can be imposed on the scalar leptoquark couplings using $\mu - e$ conversion rate. The dominant contribution to the $\mu - e$ conversion rate is obtained through considering the tree diagram shown in Fig. 2(d) which leads to the effective Lagrangian

$$\begin{aligned}\mathcal{L}_{eff}^{(u_a)} &= \sum_{a=1}^{3}\sum_{k=1}^{2} -\frac{1}{M_{S_k}^2}\Bigg[\frac{1}{2}h_{a2}h_{a1}^{*}\Gamma^{\dagger}_{S_L,k}\Gamma_{k,S_L}(\bar{e}\gamma^{\mu}P_L\mu)(\bar{u}_a\gamma_{\mu}P_Lu_a) \\ &+ \frac{1}{8}h_{a2}h_{a1}^{'*}\Gamma^{\dagger}_{S_R,k}\Gamma_{k,S_L}(\bar{e}\sigma^{\mu\nu}P_R\mu)(\bar{u}_a\sigma_{\mu\nu}P_Ru_a) \\ &- \frac{1}{2}h_{a2}h_{a1}^{'*}\Gamma^{\dagger}_{S_R,k}\Gamma_{k,S_L}(\bar{e}P_R\mu)(\bar{u}_aP_Ru_a) + (h \leftrightarrow h', R \leftrightarrow L)\Bigg], \end{aligned} \tag{36}$$

where we have used Fierz transformation for chiral fermions. $P_{R,L} = (1 \pm \gamma^5)/2$, u_a are light and heavy type-up quarks and σ matrix is defined by $\sigma^{\mu\nu} = \frac{i}{2}[\gamma^{\mu}, \gamma^{\nu}]$. The operators involving $\bar{u}_a\gamma_{\mu}\gamma_5u_a$, $\bar{u}_a\gamma_5u_a$, or $\bar{u}_a\sigma_{\mu\nu}u_a$ do not contribute to the coherent conversion processes and thus we can drop them and write

$$\begin{aligned}\mathcal{L}_{eff}^{(u_a)} &= \sum_{a=1}^{3}\Bigg[\left(C_{VR}^{(u_a)}\ \bar{e}\gamma^{\mu}P_R\mu + C_{VL}^{(u_a)}\ \bar{e}\gamma^{\mu}P_L\mu\right)\bar{u}_a\gamma_{\mu}u_a \\ &+ \left(C_{SR}^{(u_a)}\ \bar{e}P_L\mu + C_{SL}^{(u_a)}\ \bar{e}P_R\mu\right)\bar{u}_au_a\Bigg]. \end{aligned} \tag{37}$$

where we have defined

$$\begin{aligned}C_{VR}^{(u_a)} &= -h_{a2}h_{a1}^{*}\sum_{k}\frac{1}{2M_{S_K}^2}\Gamma^{\dagger}_{S_L,k}\Gamma_{k,S_L} \\ C_{SR}^{(u_a)} &= \frac{1}{2}h_{a2}h_{a1}^{'*}\sum_{k}\frac{1}{M_{S_K}^2}\Gamma^{\dagger}_{S_R,k}\Gamma_{k,S_L} \end{aligned} \tag{38}$$

$C_{VL}^{(u_a)}$ and $C_{SL}^{(u_a)}$ can be obtained by the the exchange $h \leftrightarrow h', R \leftrightarrow L$ in Eq.(38). The next step for the calculation of $\mu - e$ conversion is to match the Lagrangian in Eq.(37) to the Lagrangian at the nucleon level. Hence we integrate out the heavy quarks [24] and so the effective Lagrangian in Eq.(37) becomes

$$\begin{aligned}\mathcal{L}^{(u)}_{\text{eff}} &= \Big(C^{(u)}_{VR}\,\bar{e}\gamma^\mu P_R\mu + C^{(u)}_{VL}\,\bar{e}\gamma^\mu P_L\mu\Big)\,\bar{u}\gamma_\mu u \\ &+ \Big(C^{(u)}_{SR}\,\bar{e}P_L\mu + C^{(u)}_{SL}\,\bar{e}P_R\mu\Big)\,\bar{u}u. \end{aligned} \tag{39}$$

Then, the effective Lagrangian (39) is matched to the nucleon level Lagrangian [25] through the following replacements of the operators [23, 24]:

$$\begin{aligned}\bar{u}u &\to G^{(u,N)}_S\bar{\psi}_N\psi_N \\ \bar{u}\gamma_\mu u &\to f^{(u)}_{VN}\;\bar{\psi}_N\gamma_\mu\psi_N\ , \end{aligned} \tag{40}$$

where N represents each nucleon ($N = p, n$), ψ_N are the nucleon fields, and G, f are given by [23, 24]

$$f^{(u)}_{Vp} = 2, \qquad f^{(u)}_{Vn} = 1, \quad G^{(u,p)}_S = 5.1, \quad G^{(u,n)}_S = 4.3 \tag{41}$$

Finally, the Lagrangian at nucleon level can be written as

$$\begin{aligned}\mathcal{L}^{(N)}_{eff} = \sum_{N=p,n}\Bigg[&\Big(\tilde{C}^{(N)}_{VR}\;\bar{e}\gamma^\mu P_R\mu + \tilde{C}^{(N)}_{VL}\;\bar{e}\gamma^\mu P_L\mu\Big)\;\bar{\psi}_N\gamma_\mu\psi_N \\ &+\;\Big(\tilde{C}^{(N)}_{SR}\;\bar{e}P_L\mu + \tilde{C}^{(N)}_{SL}\;\bar{e}P_R\mu\Big)\;\bar{\psi}_N\psi_N + h.c.\Bigg]\ . \end{aligned} \tag{42}$$

where we have introduced the following redefinitions for the vector quantities:

$$\tilde{C}^{(p)}_{VR} = C^{(u)}_{VR}\;f^{(u)}_{Vp} \tag{43}$$

$$\tilde{C}^{(n)}_{VR} = C^{(u)}_{VR}\;f^{(u)}_{Vn} \tag{44}$$

$$\tilde{C}^{(p)}_{VL} = C^{(u)}_{VL}\;f^{(u)}_{Vp} \tag{45}$$

$$\tilde{C}^{(n)}_{VL} = C^{(u)}_{VL}\;f^{(u)}_{Vn}\ , \tag{46}$$

while the scalar ones read:

$$\tilde{C}^{(p)}_{SR} = C^{(u)}_{SR}\;G^{(u,p)}_S \tag{47}$$

$$\tilde{C}^{(n)}_{SR} = C^{(u)}_{SR}\;G^{(u,n)}_S \tag{48}$$

$$\tilde{C}^{(p)}_{SL} = C^{(u)}_{SL}\;G^{(u,p)}_S \tag{49}$$

$$\tilde{C}^{(n)}_{SL} = C^{(u)}_{SL}\;G^{(u,n)}_S\ . \tag{50}$$

In order to calculate the $\mu - e$ conversion amplitude we need to calculate the matrix elements of $\bar{\psi}_N \psi_N$ and $\bar{\psi}_N \gamma_\mu \psi_N$ of the transition between the initial and the final states of nucleus [23, 24]:

$$\begin{aligned}
\langle A, Z|\bar{\psi}_p \psi_p|A, Z\rangle &= Z\rho^{(p)} \\
\langle A, Z|\bar{\psi}_n \psi_n|A, Z\rangle &= (A-Z)\rho^{(n)} \\
\langle A, Z|\bar{\psi}_p \gamma^0 \psi_p|A, Z\rangle &= Z\rho^{(p)} \\
\langle A, Z|\bar{\psi}_n \gamma^0 \psi_n|A, Z\rangle &= (A-Z)\rho^{(n)} \\
\langle A, Z|\bar{\psi}_N \gamma^i \psi_N|A, Z\rangle &= 0 \, . \qquad (51)
\end{aligned}$$

where $|A, Z\rangle$ represents the nuclear ground state, with A and Z are the mass and atomic number of the isotope respectively, while $\rho^{(p)}$ and $\rho^{(n)}$ are the proton and neutron densities respectively. Finally, the $\mu - e$ conversion rate is given by [24]:

$$\begin{aligned}
\Gamma_{conv} &= \frac{m_\mu^5}{4}\left|4\left(\tilde{C}_{SR}^{(p)} S^{(p)} + \tilde{C}_{SR}^{(n)}\, S^{(n)}\right) + 4\tilde{C}_{VR}^{(p)}\, V^{(p)} + 4\tilde{C}_{VR}^{(n)}\, V^{(n)}\right|^2 \\
&+ \frac{m_\mu^5}{4}\left|4\left(\tilde{C}_{SL}^{(p)} S^{(p)} + \tilde{C}_{SL}^{(n)}\, S^{(n)}\right) + 4\tilde{C}_{VL}^{(p)}\, V^{(p)} + 4\tilde{C}_{VL}^{(n)}\, V^{(n)}\right|^2 \qquad (52)
\end{aligned}$$

where $V^{(N)}, S^{(N)}$ are dimensionless integrals representing the overlap of electron and muon wave functions weighted by appropriate combinations of protons and neutron densities [23]. For phenomenological applications, it is useful to normalize the conversion rate to the muon capture rate through the quantity:

$$B_{\mu-e}(Z) \equiv \frac{\Gamma_{conv}(Z, A)}{\Gamma_{capt}(Z, A)} \, . \qquad (53)$$

The current bounds on $B_{\mu-e}$ for Titanium atom and Gold atom obtained by SINDRUM collaboration are respectively $B_{\mu-e}(Ti) < 4.3 \times 10^{-12}$ [26], $B_{\mu-e}(Au) < 7 \times 10^{-13}$ [27] both at 90%CL. The numerical values of $V^{(N)}, S^{(N)}$ and Γ_{capt} for Titanium and Gold atoms are listed In Table I.

V. NUMERICAL RESULTS AND DISCUSSION

Let us now proceed to analyse and discuss our numerical results. The quark masses are evaluated at the energy scale $\mu = 300$ GeV [28], which is the typical leptoquark mass scale used in this work,

$$m_t = 161.4\,\text{GeV}, \quad m_c = 0.55\,\text{GeV}, \quad m_u = 11.4 \times 10^{-3}\,\text{GeV}, \qquad (54)$$

Nucleus	$S^{(p)}[m_\mu^{5/2}]$	$S^{(n)}[m_\mu^{5/2}]$	$V^{(p)}[m_\mu^{5/2}]$	$V^{(n)}[m_\mu^{5/2}]$	$\Gamma_{capture}[10^6 s^{-1}]$
Ti_{22}^{48}	0.0368	0.0435	0.0396	0.0468	2.59
Au_{79}^{197}	0.0614	0.0918	0.0974	0.146	13.07

TABLE I: Data taken from Tables I and VIII of [23].

while we use the following values for [29]

$$\alpha_{em} = 1/137.0359, \quad M_W = 80.45\,\mathrm{GeV}, \quad M_Z = 91.1875\,\mathrm{GeV}. \tag{55}$$

We assume as in Ref. [31], that all the couplings h and h' are real and equal to each other [20],

$$h = h' = h^*. \tag{56}$$

We use leptoquark mass splitting $\Delta = 500$ GeV in our analysis, where Δ is defined as $\sqrt{M_{S_2}^2 - M_{S_1}^2}$. Consequently, the remaining parameters in the leptoquark model are the mass of the light scalar leptoquark M_{S_1}, the mixing angle θ_{LQ}, and the couplings $h_{a\ell}$ (a =u, c and t). Also, we assume that the scalar leptoquark may explain the discrepancy Δa_μ between the experimentally measured muon $(g-2)_\mu$ and its SM prediction Eq. (3) and hence this condition restricts the possible range of the parameters. We have performed a scan over all the input parameters, $M_{S_1} \leq 1500$ GeV, $-1 \leq \sin\theta_{LQ} \leq 1$ and $\alpha_{em} \leq |h_{q\mu}|^2 \leq 1$. Then, after imposing all the existing constraints arising from π leptonic decays and direct search, we select all sets of the input parameters producing the same values for $(g-2)_\mu$ at 1σ range of data.

In Fig. 3, we show the allowed regions for different type-up quarks contributions which are compatible with $a_\mu^{LQ} = \Delta a_\mu$ at 1σ range of data where the red color (green color) region corresponds to top-quark (charm-quark) contribution respectively. As can be seen from the left panel of Fig. 3, the dominant contribution is around $\sin 2\theta_{LQ} \sim 0.7$ for both top and charm quarks. In addition, we find that, sizeable scalar leptoquark effects to the $(g-2)_\mu$ at 1σ are obtained for the values of M_{S_1} which satisfy $M_{S_1} \approx 1$ TeV for top quark contribution and $M_{S_1} \approx 400$ GeV for charm quark contribution. We note also that it is not possible to use the up quark loop contributions alone for LQ, since the couplings $|h_{u\mu}|$ are strongly constrained by the π leptonic decays. It has been found that the LHC has the potential to discover light scalar LQ with a mass up to 1.2 TeV and where the Yukawa coupling are equal to the electromagnetic coupling [30].

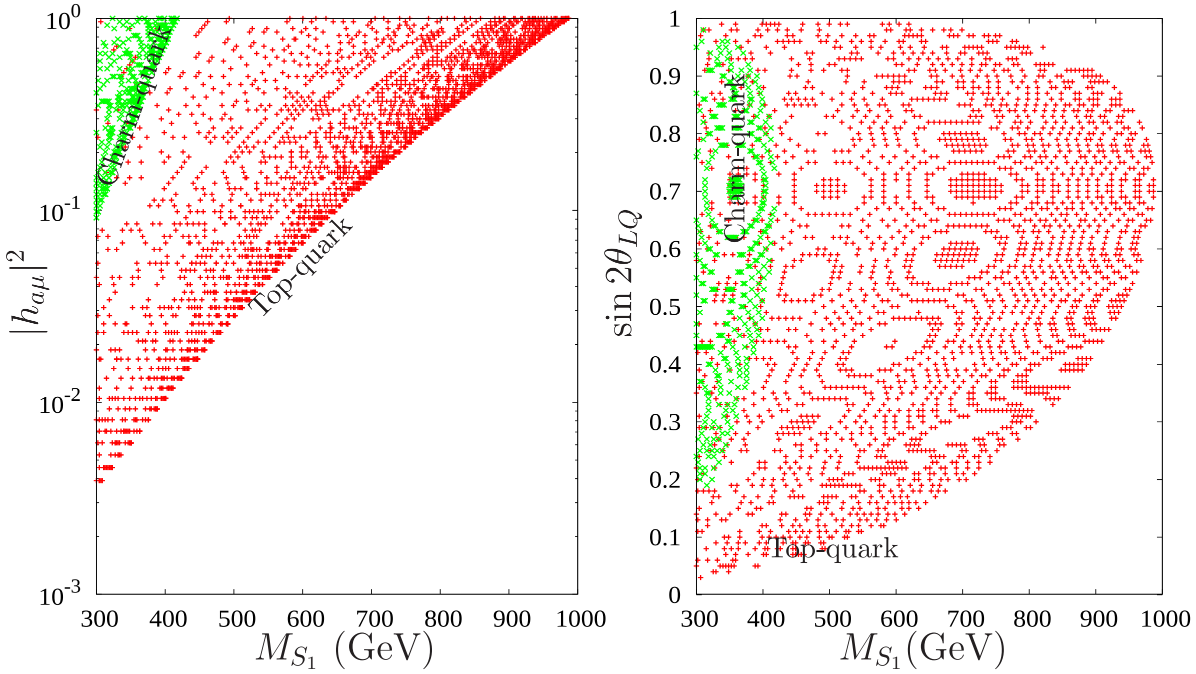

FIG. 3: The allowed regions on the $(M_{S_1} - |h_{a\mu}|^2)$ plane (left) and on the $(M_{S_1} - \sin 2\theta_{LQ})$ plane (right) for top-quark (red color) and charm-quark (green color) contributions, taking into account $a_\mu^{LQ} = \Delta a_\mu$ at 1σ.

In order to find the constraints on the combination of LQ couplings we require that each individual LQ coupling contribution to the branching ratio does not exceed the experimental current limits on the $\mathrm{Br}(\ell \to \ell' \gamma)$ (2) and $\mu - e$ conversion in nuclei. The latter process is used to set the strongest constraints on the product $h_{u\mu} h_{ue}$ which involve the first generation, since, in this case, the process is induced at tree-level. On the other hand, the $\ell \to \ell' \gamma$ decays which are induced at one-loop by the photon-penguins, Z-penguins and box diagrams [see Figs. 2(a)-2(c)], allow us to constrain the complementary combinations of the couplings involving the second and third generation of quarks, namely $h_{a\ell} h_{a\ell'}$, where a = c, t. The $\mu - e$ conversion process can be also used to set constraints on the second and third quark generations. However, we stress that the bounds from the $\mu - e$ conversion are suffering from being model-dependent due to the non perturbative calculations of the nuclear form factors, while the bounds which are obtained from the $\ell \to \ell' \gamma$ decays are not. Taking into account $(g-2)_\mu$ constraint, and experimental upper limits on the $(\mu - e)_{Ti,Au}$ conversion rates [26, 27] at 90%CL., we obtain the following upper bounds

$$h_{u\mu}h_{ue} \leq 4.38 \times 10^{-6} \tag{57}$$

for Titanium atom while for Gold atom the bound reads

$$h_{u\mu}h_{ue} \leq 6.25 \times 10^{-6} \tag{58}$$

Clearly, the bounds obtained for both Titanium and Gold atoms are of the same order and severely constraint the product of the leptoquark couplings $h_{u\mu}h_{u\mu}$. Our results are consistent with the effective Hamiltonian and approximation used in Ref. [31]. The products of the couplings $h_{a\ell}h_{a\ell'}$ where a=c,t and $\ell, \ell' = \tau, \mu, e$, appear only at the one-loop level contribution to the $\tau \to (\mu, e)\gamma$ and $\mu \to e\gamma$ decays. Therefore, they could be larger if they are compared with $h_{u\mu}h_{ue}$ ones without violating the experimental upper limits on the branching ratios. The bounds obtained on these combinations of couplings in the muon sector are given by

$$h_{c\mu}h_{ce} \leq 1.22 \times 10^{-3}, \quad h_{t\mu}h_{te} \leq 5.73 \times 10^{-3} \tag{59}$$

while for the tau sector they become

$$h_{c\tau}h_{c\mu} \leq 4.78 \times 10^{-3}, \quad h_{t\tau}h_{t\mu} \leq 8.13 \times 10^{-3}, \tag{60}$$

$$h_{c\tau}h_{ce} \leq 7.8 \times 10^{-1}, \quad h_{t\tau}h_{te} \leq 8.0 \times 10^{-1}, \tag{61}$$

In the following studies of the τ and μ LFV processes, we will use the parameter space which is discussed above. We start by investigating the LFV τ and μ decay processes generated by the same LQ-scalar interactions as those of $(g-2)_\mu$. At one-loop level, the LQ-scalar gives contributions to the $\tau^- \to \mu^-\mu^-\mu^+$, $\tau^- \to e^-e^-e^+$, by means of the so-called γ- and Z- penguins and box diagrams.

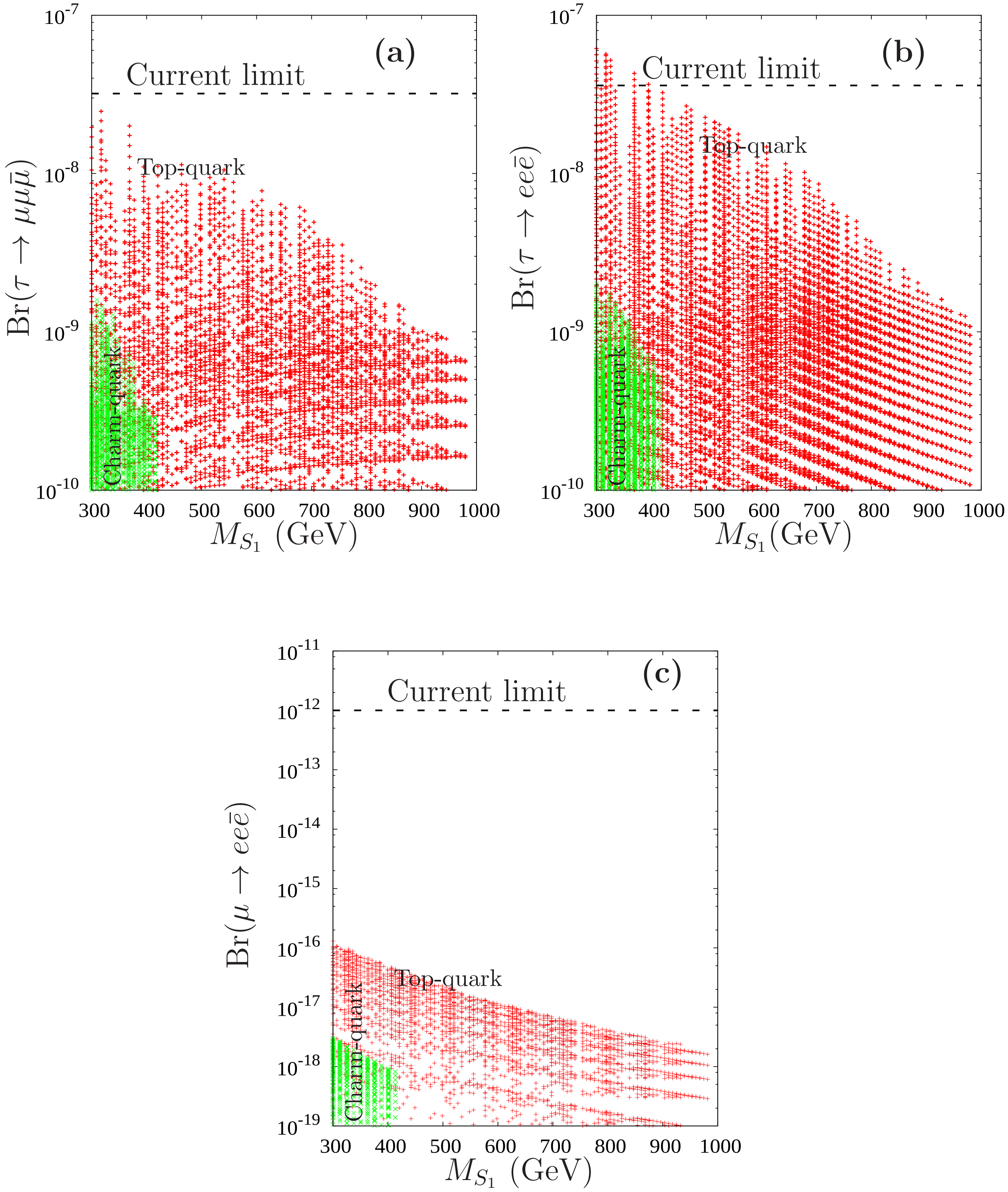

FIG. 4: Scatter plots of (a) $\mathrm{Br}(\tau \to \mu\mu\bar{\mu})$, (b) $\mathrm{Br}(\tau \to ee\bar{e})$ and (c) $\mathrm{Br}(\mu \to ee\bar{e})$ as a function of light leptoquark mass M_{S_1} for top-quark (red color) and charm-quark (green color) contributions. The horizontal lines of each plot are the current limits of τ and μ LFV decay branching ratios.

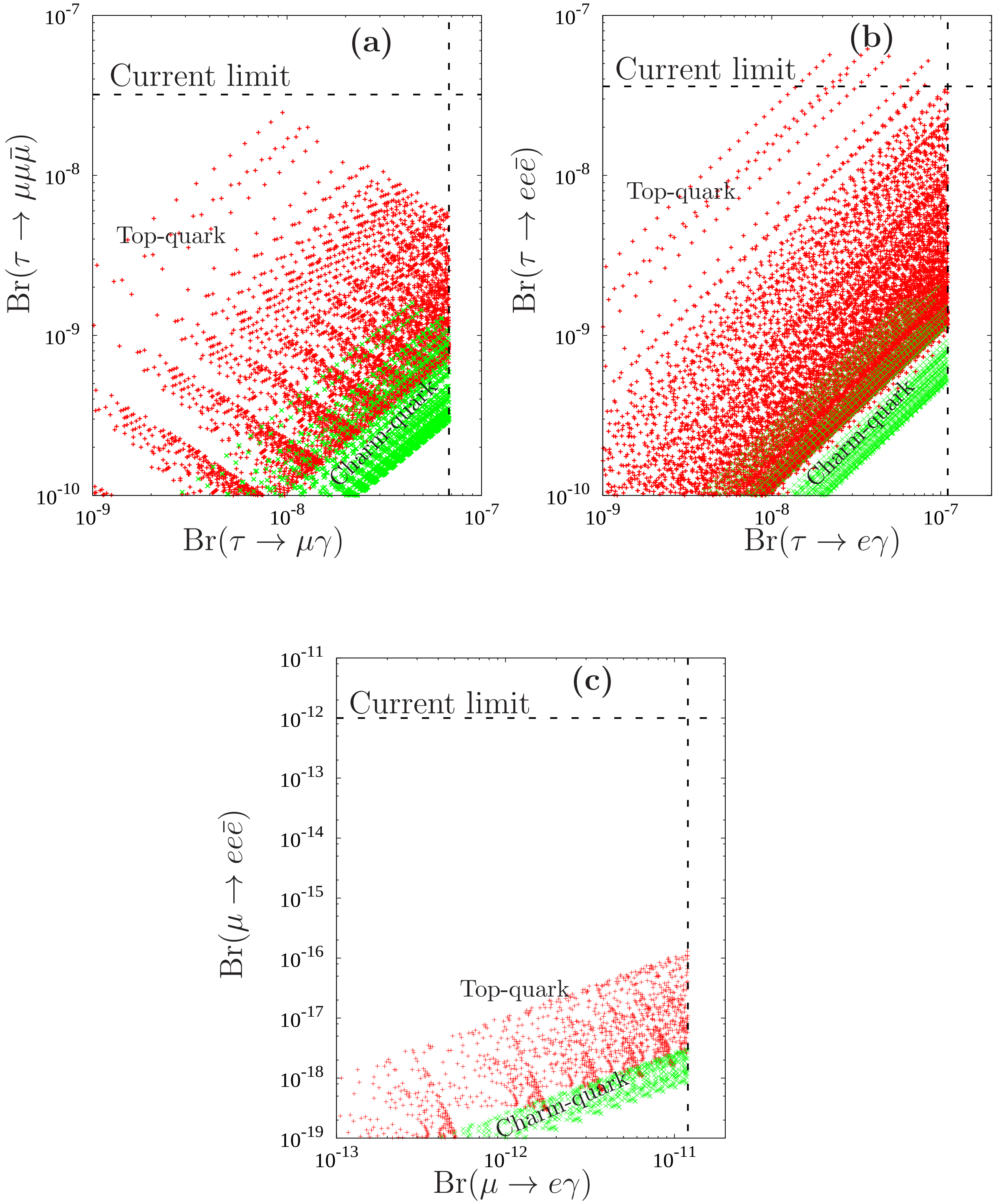

FIG. 5: Correlations between (a) $\mathrm{Br}(\tau \to \mu\mu\bar{\mu})$ and $\mathrm{Br}(\tau \to \mu\gamma)$, (b) $\mathrm{Br}(\tau \to ee\bar{e})$ and $\mathrm{Br}(\tau \to e\gamma)$, (c) $\mathrm{Br}(\mu \to ee\bar{e})$ and $\mathrm{Br}(\mu \to e\gamma)$. for top-quark (red color) and charm-quark (green color) contributions The vertical and horizontal lines correspond to the upper limits of τ and μ LFV decay branching ratios.

In Figs 4, we present our predictions for the branching ratios of ($\tau \to \mu\mu\bar{\mu}$) (a) and ($\tau \to ee\bar{e}$) (b) as a function of light LQ mass M_{S_1} for top-quark (red color) and charm-quark (green color) contributions. These plots have origin in $M_{S_1} = 300$ GeV which roughly corresponds to the exclusion limit obtained at HERA [15] for leptoquark masses with couplings of electromagnetic strenght. As we can see the main contribution comes from the top-quark contribution and can reach 2.47 $\times 10^{-8}$ for Br($\tau \to 3\mu$) and 5.66 $\times 10^{-8}$ for Br($\tau \to 3e$) which are comparable with the present bounds. We find that the main contribution to $\tau \to ee\bar{e}$ and $\tau \to \mu\mu\bar{\mu}$ decays is produced from the photon-penguins diagrams which were not taken into account in Ref. [31]. In fact, for large LQ mass ($m_q \ll M_{S_1}$), the photon-penguins are proportional to $h^2 \log(m_q/M_{S_1})/M_{S_1}^2$ which were known as log enhancement in the literature [32]. On the other hand, the naive expectation of Z-penguin and box diagrams leads to that they are of orders $\mathcal{O}(h^2 m_q^2/M_{S_1}^4)$ and $\mathcal{O}(h^4 m_q^2/M_{S_1}^4)$, respectively. The same considerations regarding log enhancements hold for the $\tau \to e\mu^-\mu^+$ and $\tau \to \mu e^- e^+$ processes. However, the uppper limits on the Brs of $\tau \to e\mu^-\mu^+$ and $\tau \to \mu e^- e^+$ could be of $\mathcal{O}(10^{-8})$ and the order in size is Br($\tau \to 3e$) > Br($\tau \to \mu^- e^- e^+$) > Br($\tau \to e^- \mu^- \mu^+$) > Br($\tau \to 3\mu$). Since, $\tau \to e^- e^- \mu^+$ and $\tau \to \mu^- \mu^- e^+$ are induced by box diagrams then they are expected to be small. On the contrary, since the current bound on the $\mu \to e\gamma$ decay imposes very strong constraints on the related couplings, the predicted Br($\mu \to 3e$) is rather too small to be observed.

In Fig. 5, we show the correlations between Br($\tau \to 3\mu$) and Br($\tau \to \mu\gamma$) in the upper left panel, (b) Br($\tau \to 3e$) and Br($\tau \to e\gamma$) in the upper right panel, and (c) Br($\mu \to 3e$) and Br($\mu \to e\gamma$) in the lower panel. We observe that it is possible to accommodate both $\tau \to 3\ell$ and $\tau \to \ell\gamma$ branching ratios for certain choices of LQ parameters. This leads to simple correlation like

$$\frac{Br(\tau \to 3\ell)}{Br(\tau \to \ell\gamma)} \approx \mathcal{O}(10^{-1}), \qquad \frac{Br(\mu \to 3e)}{Br(\mu \to e\gamma)} \approx \mathcal{O}(10^{-3}) \tag{62}$$

for top-quark contribution, which is in agreement with the ratio expected by the dominance of the Penguin-type Fig.2(a)-(b).

VI. CONCLUSION

We have studied the muon anomalous magnetic moment, lepton flavor violating muon and tau decays $\ell \to \ell_i \ell_j \bar{\ell}_j$ and $\ell \to \ell' \gamma$ that are generated by scalar LQ interactions. We have found that scalar LQ can explain the discrepancy between the experimental value of $(g-2)_\mu$ and its standard model prediction without any contradictions with the experimental bound of LFV tau decay processes. The present experimental limits are used to constrain the leptoquark parameter space. We set equal couplings and obtain the upper limits of the different product of leptoquark couplings by confronting LFV observable with experimental results. Our prediction is that $\tau \to 3\mu, 3e, e2\mu$ and $\tau \to \mu 2e$ get the leading contributions from the so-called photon-penguin diagrams and could be of $\mathcal{O}(10^{-8})$ which can be accessible by the presents experiments and the future linear colliders, such as ILC. On the contrary, the current bounds on LFV impose very strong constraints on the $\mathrm{Br}(\mu \to ee\bar{e})$ and the ratio is too small to be observed in the near future. Hence any observation of LFV processes in the charged lepton sector, which are being probed with ever increasing sensitivity, would unambiguously point to non-standard interactions. Indeed, such indirect observations taken in isolation may not imply much on the exact nature of new physics. But a study of possible correlations of its effects on different independently measured charged LFV observable might provide a powerful cross-check and lead to identification of new physics through LHC/LFV synergy.

ACKNOWLEDGEMENTS

We would like to thank the Abdus Salam International Centre for Theoretical Physics (ICTP) for good hospitality and acknowledge the considerable help of the High Energy Section. This work was done at the high energy section within the framework of the associate Scheme. We would like also thank Chuan-Hung Chen for useful discussions and comments. R.B. was supported by National Cheng Kung University Grant No. HUA 97-03-02-063.

Appendix A: Constraint form $\pi \to e\nu_e$ and $\pi \to \mu\nu_\mu$ decays

We follow [33, 34] to constrain leptoquark parameters using pion decay data. Form the interactions given in Eq. (4), we obtain the effective four-Fermi interaction

$$\begin{aligned}\mathcal{L}_{eff} &= -\frac{h'_{ai}h'^{*}_{bj}\Gamma^{+}_{R,k}\Gamma_{k,R}}{M^2_{S_k}}(\bar{e}^c_i P_L u_a)(\bar{d}_b P_R \nu^c_j) \\ &- \frac{h_{ai}h'^{*}_{bj}\Gamma^{\dagger}_{R,k}\Gamma_{k,L}}{M^2_{S_k}}(\bar{e}^c_i P_R u_a)(\bar{d}_b P_R \nu^c_j)\end{aligned} \tag{A1}$$

By using the Fierz transformation, we can rewrite Eq.(A1) as

$$\begin{aligned}\mathcal{L}_{eff} &= -\frac{1}{2M^2_{S_k}}h'_{ai}h'^{*}_{bj}\Gamma^{\dagger}_{R,k}\Gamma_{k,R}(\bar{d}_{L,b}\gamma_\mu u_{L,a})(\bar{\nu}_{L,j}\gamma^\mu e_{L,i}) \\ &+ \frac{1}{2M^2_{S_k}}h_{ai}h'^{*}_{bj}\Gamma^{\dagger}_{R,k}\Gamma_{k,L}(\bar{d}_{L,b}u_{R,a})(\bar{\nu}_{L,j}e_{R,i})\end{aligned} \tag{A2}$$

On the other hand, the conventional interaction for the $\pi \to l\nu_l$ decay in the SM is given by

$$\mathcal{L}_{eff} = -\frac{G_F V_{ud}}{\sqrt{2}}[\bar{\nu}\gamma_\mu(1-\gamma_5)l][\bar{d}\gamma^\mu(1-\gamma_5)u] + \text{h.c}$$

here $|V_{ud}|$ is the Cabibbo-Kobayashi-Maskawa (CKM) matrix elements between the constituent of the pion meson and G_F is the Fermi coupling constant. The ratio R_{th} of the electronic and muonic decay modes is [35]

$$\begin{aligned}R_{th} &= \frac{\Gamma_{SM}(\pi^+ \to \bar{e}\nu_e)}{\Gamma_{SM}(\pi^+ \to \bar{\mu}\nu_\mu)} \\ &= \left(\frac{m^2_e}{m^2_\mu}\right)\left(\frac{m^2_\pi - m^2_e}{m^2_\pi - m^2_\mu}\right)^2\left(1+\delta\right) \\ &= (1.2352 \pm 0.0001) \times 10^{-4}\end{aligned} \tag{A3}$$

where δ is the radiative corrections, Thus the ratio R_{th} is very sensitive to non standard model effects (such as multi-Higges, non-chiral leptoquarks). The experimental value of the ratio is [29]

$$R_{exp} = (1.2302 \pm 0.004) \times 10^{-4} \tag{A4}$$

The interference between the standard model and LQ model can be expressed by

$$R_{SM-LQ} = R_{th} + R_{th}\,\frac{m^2_{\pi^+}}{m_u + m_d}\left(\frac{1}{\sqrt{2}}\frac{\text{Re}(h_{ue}h'^{*}_{ue})}{G_F V_{ud} M^2_{S_k}}\frac{1}{m_e} - \frac{1}{\sqrt{2}}\frac{\text{Re}(h_{u\mu}h'^{*}_{u\mu})}{G_F V_{ud} M^2_{S_k}}\frac{1}{m_\mu}\right)\Gamma^{\dagger}_{R,k}\Gamma_{k,L} \tag{A5}$$

At 2σ level, we get

$$R_{min} < \sum_{k=1}^{2}\left(\frac{m_\pi}{m_e}\frac{\mathrm{Re}(h_{ue}h_{ue}^{'*})}{M_{S_k}^2} - \frac{m_\pi}{m_\mu}\frac{\mathrm{Re}(h_{u\mu}h_{u\mu}^{'*})}{M_{S_k}^2}\right)\Gamma^\dagger_{R,k}\Gamma_{k,L} < R_{max} \tag{A6}$$

where,

$$R_{min} = -1.06\times 10^{-8}\mathrm{GeV}^{-2}, \tag{A7}$$

$$R_{max} = 2.45\times 10^{-9}\mathrm{GeV}^{-2}. \tag{A8}$$

The total contribution to R_{SM-LQ} must be smaller than the differences between SM and experiment within the allowed error limits.

Appendix B: One loop functions

The loop functions used in text are given by

$$F_1(x) = \frac{\left[2+3x-6x^2+x^3+6x\log(x)\right]}{12(1-x)^4}, \tag{B1}$$

$$F_2(x) = \frac{\left[1-6x+3x^2+2x^3-6x^2\log(x)\right]}{12(1-x)^4}, \tag{B2}$$

$$F_3(x) = \frac{-1}{2(1-x)^3}\left[3-4x+x^2+2\log(x)\right], \tag{B3}$$

$$F_4(x) = \frac{1}{2(1-x)^3}\left[1-x^2+2x\log(x)\right], \tag{B4}$$

$$F_5(x) = \frac{1}{36(x-1)^4}\left[16-45x+36x^2-7x^3+6(2-3x)\log(x)\right] \tag{B5}$$

$$F_6(x) = \frac{\left[-2+9x-18x^2+11x^3-6x^3\log(x)\right]}{36(x-1)^4} \tag{B6}$$

$$F_7(x) = \frac{1-x+\log(x)}{(x-1)^2} \tag{B7}$$

$$F_8(x) = \frac{1}{8(x-1)^2}\left[3-4x+x^2+4x\log(x)-2x^2\log(x)\right] \tag{B8}$$

$$
\begin{aligned}
D_0(x,y,z,k) &= -\frac{x\log(x)}{(x-k)(x-y)(x-z)} - \frac{y\log(y)}{(y-k)(y-x)(y-z)} \\
&- \frac{z\log(z)}{(z-k)(z-x)(z-y)} - \frac{k\log(k)}{(k-x)(k-y)(k-z)}
\end{aligned} \tag{B9}
$$

$$
\begin{aligned}
D_0(y,y,z,k) &= \frac{1}{(k-y)^2(k-z)(y-z)^2}\Big[-k\log(k)(y-z)^2 + \big(-zk^2 \\
&+ \left(y^2+z^2\right)k - y^2 z\big)\log(y) \\
&+ (k-y)((k-z)(y-z) + (k-y)z\log(z))\Big]
\end{aligned} \tag{B10}
$$

$$
\begin{aligned}
D_0(x,y,k,k) &= \frac{1}{(k-x)^2(k-y)^2(x-y)}\left[-x\log(x)(k-y)^2 \right. \\
&+ (x-y)\left(k^2-xy\right)\log(k) - (k-x)((k-y)(x-y) \\
&\left. + (x-k)y\log(y))\right]
\end{aligned} \tag{B11}
$$

$$
\begin{aligned}
\widetilde{D}_0(x,y,z,k) &= -\frac{x^2\log(x)}{(x-k)(x-y)(x-z)} - \frac{y^2\log(y)}{(y-k)(y-x)(y-z)} \\
&- \frac{z^2\log(z)}{(z-k)(z-x)(z-y)} - \frac{\log(k)k^2}{(k-x)(k-y)(k-z)}
\end{aligned} \tag{B12}
$$

$$
\begin{aligned}
\widetilde{D}_0(y,y,z,k) &= \frac{1}{(k-y)^2(k-z)(y-z)^2}\left[-k^2\log(k)(y-z)^2 \right. \\
&+ y(k-z)(k(y-2z)+yz)\log(y) \\
&\left. + (k-y)\left((k-y)\log(z)z^2 + y(k-z)(y-z)\right)\right]
\end{aligned} \tag{B13}
$$

$$
\begin{aligned}
\widetilde{D}_0(x,y,k,k) &= \frac{1}{(k-x)^2(k-y)^2(x-y)}\left[-x^2\log(x)(k-y)^2 \right. \\
&+ k(x-y)(k(x+y)-2xy)\log(k) \\
&\left. - (k-x)\left((x-k)\log(y)y^2 + k(k-y)(x-y)\right)\right]
\end{aligned} \tag{B14}
$$

[1] Y. Miyazaki *et al.* [Belle Collaboration], Phys. Lett. B **660**, 154 (2008) [arXiv:0711.2189 [hep-ex]]. B. Aubert *et al.* [BABAR Collaboration], Phys. Rev. Lett. **99**, 251803 (2007)[arXiv:0708.3650 [hep-ex]]. B. Aubert *et al.* [BABAR Collaboration], Phys. Rev. Lett. **92**, 121801 (2004)[arXiv:hep-ex/0312027].

[2] M. Giffels, J. Kallarackal, M. Kramer, B. O'Leary and A. Stahl, Phys. Rev. D **77** (2008) 073010 [arXiv:0802.0049 [hep-ph]].

[3] U. Bellgardt *et al.* [SINDRUM Collaboration], Nucl. Phys. B **299**, 1 (1988).

[4] B. Aubert *et al.* [BABAR Collaboration], Phys. Rev. Lett. **95**, 041802

(2005)[arXiv:hep-ex/0502032].

[5] B. Aubert *et al.* [BABAR Collaboration], Phys. Rev. Lett. **96**, 041801 (2006) [arXiv:hep-ex/0508012].

[6] M. L. Brooks *et al.* [MEGA Collaboration], Phys. Rev. Lett. **83**, 1521 (1999)[arXiv:hep-ex/9905013].

[7] G. W. Bennett *et al.* [Muon G-2 Collaboration], Phys. Rev. D **73**, 072003 (2006)[arXiv:hep-ex/0602035].

[8] W. M. Yao *et al.* [Particle Data Group], J. Phys. G **33** (2006) 1.

[9] J. P. Miller, E. de Rafael and B. L. Roberts, Rept. Prog. Phys. **70**, 795 (2007) [arXiv:hep-ph/0703049]. F. Jegerlehner and A. Nyffeler, arXiv:0902.3360 [hep-ph]. M. Passera, W. J. Marciano and A. Sirlin, AIP Conf. Proc. **1078**, 378 (2009) [arXiv:0809.4062 [hep-ph]].

[10] M. Passera, W. J. Marciano and A. Sirlin, Phys. Rev. D **78**, 013009 (2008) [arXiv:0804.1142 [hep-ph]].

[11] A. Czarnecki and W. J. Marciano, Phys. Rev. D **64**, 013014 (2001) [arXiv:hep-ph/0102122]. F. Jegerlehner, Acta Phys. Polon. B **38**, 3021 (2007) [arXiv:hep-ph/0703125]. C. Biggio, Phys. Lett. B **668**, 378 (2008) [arXiv:0806.2558 [hep-ph]]. A. Hektor, Y. Kajiyama and K. Kannike, Phys. Rev. D **78**, 053008 (2008) [arXiv:0802.4015 [hep-ph]]. H. Chavez and J. A. Martins Simoes, Nucl. Phys. B **783**, 76 (2007) [arXiv:hep-ph/0610231].

[12] J. R. Ellis, S. Heinemeyer, K. A. Olive, A. M. Weber and G. Weiglein, JHEP **0708**, 083 (2007) [arXiv:0706.0652 [hep-ph]]. D. Stockinger, J. Phys. G **34**, R45 (2007) [arXiv:hep-ph/0609168]. A. Dedes and H. E. Haber, JHEP **0105**, 006 (2001) [arXiv:hep-ph/0102297].

[13] I. I. Y. Bigi, G. Kopp and P. M. Zerwas, Phys. Lett. B **166**, 238 (1986).

[14] J. C. Pati and A. Salam, Phys. Rev. D **10**, 275 (1974) [Erratum-ibid. D **11**, 703 (1975)]. H. Georgi and S. L. Glashow, Phys. Rev. Lett. **32**, 438 (1974). W. Buchmuller and D. Wyler, Phys. Lett. B **177**, 377 (1986).

[15] S. M. Wang [CDF Collaboration and D0 Collaboration], arXiv:hep-ex/0405075. R. Barate *et al.* [ALEPH Collaboration], Eur. Phys. J. C **12**, 183 (2000) [arXiv:hep-ex/9904011]. P. Abreu *et al.* [DELPHI Collaboration], Phys. Lett. B **446**, 62 (1999) [arXiv:hep-ex/9903072]. M. Acciarri *et al.* [L3 Collaboration], Phys. Lett. B **489** (2000) 81 [arXiv:hep-ex/0005028]. G. Abbiendi *et al.* [OPAL Collaboration], Phys. Lett. B **526**, 233 (2002) [arXiv:hep-ex/0112024]. G. Abbiendi *et al.* [OPAL Collaboration], Eur. Phys. J. C **31**, 281 (2003)

[arXiv:hep-ex/0305053]. S. Chekanov *et al.* [ZEUS Collaboration], Phys. Rev. D **68**, 052004 (2003) [arXiv:hep-ex/0304008].

[16] V. A. Mitsou, N. C. Benekos, I. Panagoulias and T. D. Papadopoulou, Czech. J. Phys. **55**, B659 (2005) [arXiv:hep-ph/0411189].

[17] S. Abdullin and F. Charles, Phys. Lett. B **464**, 223 (1999) [arXiv:hep-ph/9905396].

[18] Y. Okada, K. i. Okumura and Y. Shimizu, Phys. Rev. D **61** (2000) 094001 [arXiv:hep-ph/9906446]. K. S. Babu and C. Kolda, Phys. Rev. Lett. **89**, 241802 (2002) [arXiv:hep-ph/0206310]. B. M. Dassinger, T. Feldmann, T. Mannel and S. Turczyk, JHEP **0710**, 039 (2007) [arXiv:0707.0988 [hep-ph]]. A. G. Akeroyd, M. Aoki and Y. Okada, Phys. Rev. D **76**, 013004 (2007) [arXiv:hep-ph/0610344]. A. Arhrib, R. Benbrik and C. H. Chen, arXiv:0903.1553 [hep-ph]. R. Benbrik and C. H. Chen, Phys. Lett. B **672**, 172 (2009) [arXiv:0807.2373 [hep-ph]]. A. G. Akeroyd, M. Aoki and H. Sugiyama, Phys. Rev. D **79**, 113010 (2009) [arXiv:0904.3640 [hep-ph]].

[19] R. Benbrik and C. K. Chua, Phys. Rev. D **78**, 075025 (2008) [arXiv:0807.4240 [hep-ph]].

[20] C. K. Chua, X. G. He and W. Y. Hwang, Phys. Lett. B **479**, 224 (2000) [arXiv:hep-ph/9905340].

[21] W. Buchmuller, R. Ruckl and D. Wyler, Phys. Lett. B **191**, 442 (1987) [Erratum-ibid. B **448**, 320 (1999)].

[22] J. Hisano, T. Moroi, K. Tobe and M. Yamaguchi, Phys. Rev. D **53**, 2442 (1996) [arXiv:hep-ph/9510309].

[23] R. Kitano, M. Koike and Y. Okada, Phys. Rev. D **66** (2002) 096002 [Erratum-ibid. D **76** (2007) 059902] [arXiv:hep-ph/0203110].

[24] V. Cirigliano, R. Kitano, Y. Okada and P. Tuzon, Phys. Rev. D **80**, 013002 (2009)ibitem-Bertl:2006up [arXiv:0904.0957 [hep-ph]].W. Bertl *et al.* [SINDRUM II Collaboration], Eur. Phys. J. C **47** (2006) 337.

[25] T. S. Kosmas, S. Kovalenko and I. Schmidt, Phys. Lett. B **511**, 203 (2001)ibitem-Dohmen:1993mp [arXiv:hep-ph/0102101].C. Dohmen *et al.* [SINDRUM II Collaboration.], Phys. Lett. B **317** (1993) 631.

[26] C. Dohmen *et al.* [SINDRUM II Collaboration.], Phys. Lett. B **317** (1993) 631.

[27] W. Bertl *et al.* [SINDRUM II Collaboration], Eur. Phys. J. C **47** (2006) 337.

[28] N. Gray, D. J. Broadhurst, W. Grafe and K. Schilcher, Z. Phys. C**48**(1990) 673;

K. G. Chetyrkin and M. Steinhauser, Phys. Rev. Lett **83** (1999) 4001; *ibid.* Nucl. Phys. B**573** (2000) 617; S. G. Gorishny, A. L. Kataev, S .A .Larin and L. R. Surguladze, Mod. Phys. Lett. A**5**(1990)2703,*ibid.* Phys. Rev. D**43** (1991) 1633.

[29] W. M. Yao et *al* Particle Data Group, J. Phys. G**30**, 1 (2006) and 2007 partial update for the 2008 edition.

[30] A. Belyaev, C. Leroy, R. Mehdiyev and A. Pukhov, JHEP **0509**, 005 (2005) [arXiv:hep-ph/0502067]. B. Dion, L. Marleau, G. Simon and M. de Montigny, Eur. Phys. J. C **2**, 497 (1998) [arXiv:hep-ph/9701285]. J. L. Hewett and S. Pakvasa, Phys. Rev. D **37**, 3165 (1988).

[31] S. Davidson, D. C. Bailey and B. A. Campbell, Z. Phys. C **61**, 613 (1994) [arXiv:hep-ph/9309310].

[32] Y. Kuno and Y. Okada, Rev. Mod. Phys. **73**, 151 (2001) [arXiv:hep-ph/9909265]. W. J. Marciano and A. I. Sanda, Phys. Rev. Lett. **38**, 1512 (1977).

[33] O. U. Shanker, Nucl. Phys. B **204**, 375 (1982).

[34] S. Davidson, D. Bailey and A. Campbell, Z.Phys. C**61**, 613 (1994).

[35] V. Cirigliano and I. Rosell, Phys. Rev. Lett. **99**, 231801 (2007) [arXiv:0707.3439 [hep-ph]].